International Journal of Bifurcation and Chaos, Vol. 1, No. 1 (1991) 227–234

ORDER AND CHAOS IN THE TORAL LOGISTIC LATTICE

RALPH H. ABRAHAM
Department of Mathematics, University of California, Santa Cruz, CA 95064, USA

JOHN B. CORLISS
NRC Senior Resident Research Associate, Computer Systems Research Facility, NASA Goddard Space Flight Center, Greenbelt, MD 20771, USA

JOHN E. DORBAND
Computer Systems Research Facility, NASA Goddard Space Flight Center, Greenbelt, MD 20771, USA

Received July 19, 1990; Revised August 6, 1990

Cellular dynamical systems, alias lattice dynamical systems, emerged as a new mathematical structure and modeling strategy in the 1980s. Based, like cellular automata, on finite difference methods for partial differential equations, they provide challenging patterns of spatiotemporal organization, in which chaos and order cooperate in novel ways. Here we present initial findings of our exploration of a two-dimensional logistic lattice with the Massively Parallel Processor (MPP) at NASA's Goddard Space Flight Center, a machine capable of 200 megaflops per second. A video tape illustrating these findings is available.

1. Introduction

Cellular dynamical systems (also known as cellular dynamata or lattice dynamical systems) are a class of mathematical structures belonging to the larger class of cellular automata, and providing a wealth of spatio-temporal patterns in a context indexed by continuous parameters. Neural nets, for example, may be regarded as cellular dynamical systems. Recalling the concepts of cellular dynamical systems, we are concerned with spatial lattices of identical dynamical schemes called *standard cells* [Abraham, 1986]. A *dynamical scheme* is a parametrized family of dynamical systems. The parameters are called *controls*, while the dynamics evolve in a space of *states*. Just as a dynamical system is visualized by its *phase portrait*, a dynamical scheme is visualized by its *response diagram*. For an encyclopedia of response diagrams, see Part Four of Abraham [1982–88]. When possible, we think of these as families of phase portraits, lined up with the state spaces vertical and the control parameters horizontal. In the spatial lattice, the cells are coupled by *coupling schemes*. Usually, these are functions from the states at one node to the controls at another node. The functions may depend on their own control parameters. In simple cases, each node is coupled to its nearest neighbors only. In more complex cases, such as neural nets, each node may be coupled to every other node. In mathematical theory, there are three important categories of dynamical system: iterated functions, iterated diffeomorphisms, and continuous flows defined by a vector field. In digital computation, these distinctions tend to break down.

In this paper, we concentrate on a single model: a cellular dynamical system comprising a two-dimensional lattice on the torus of 128 by 128 nodes, with a logistic map at each site. The coupling is to nearest neighbors only, by the simple coupling scheme known as *Laplacian coupling*, explained in Sec. 2 below. The logistic equation dates from Verhulst in 1838. This type of cellular dynamaton corresponds to a partial differential equation which occurs in the literature for the first time, as far as we know, in 1930, in Roland Fisher's model for the spread of mutant genes in a Petri dish of fruit flies [Fisher, 1930/1958]. Since 1980, there has been a growing literature of experimental results,

particularly for strings (one-dimensional lattices) of logistic maps. These maps provide the simplest examples of a chaotic dynamical system, and were popularized through the pioneering work of Robert May [1976]. The theory is well organized in a recent textbook [Devaney, 1989]. For a recent survey of results on one-dimensional logistic lattices, see Crutchfield [1987]. Following the wave of interest in the chaotic behavior of the iterated logistic function itself, and the availability of computers capable of fast arithmetic, came the pioneering work of Crutchfield, Kaneko, and others, on logistic strings, in 1983. Experiments with two-dimensional lattices have been inhibited by their enormous computational cost. But preliminary results have been very exciting. (Read Karpral [1986], Kaneko [1989] and, if possible, try to see Shaw [1988] and Crutchfield [1984]). Two-dimensional cellular automata (CAs) are rather less expensive to compute than are two-dimensional cellular dynamata (CDs), and an inexpensive CA board for personal computers is available from Systems Concepts, San Francisco, CA. However, CAs are more difficult to utilize in modeling than are the CDs which we describe in this paper. A fascinating property of these cellular dynamata is their ability to organize an ensemble of chaotic systems into a pattern with recognizable and stable large-scale features. We see this as a significant property from the point of view of morphogenesis in complex natural systems, such as a global ecosystem, an embryo, an immune system, a brain, a society, or the origin of life. In this paper, we introduce the conditions of our experiment, and describe the phenomenology discovered in our initial exploration. The MPP and the Blue Room allow us to compute at about one hundred times the rate of the early explorers.

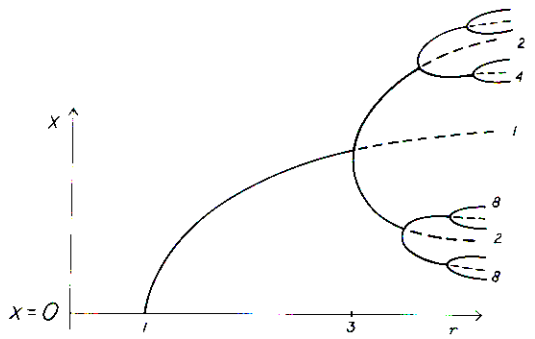

Fig. 1. The bifurcation diagram of the logistic map. Fixing a value of the bifurcation parameter, r, on the horizontal axis and an initial value, x_0, on the vertical axis, we iterate the map until the trajectory, $x_0, x_1 = f(x_0), \ldots$, converges to an attractor. The attractors found in this way are shown here in solid black, the *locus of attraction*. The dashed curves show the locus of repulsion. For the values of r well below 4, the attractors are all periodic trajectories. Here we see periods one, two, four, and eight. Each bifurcation is a period-doubling octave jump. More details may be found in Devaney [1989].

2. The Toral Logistic Lattice

The dynamical scheme employed as the standard cell in this work comprises the iteration of the function:

$$\text{controls: } (r, c) \in C \subset \mathbb{R}^2 \text{, both nonnegative ,} \quad (2.1a)$$

$$\text{states: } x \in [0, 1] \subset \mathbb{R} \text{, the unit interval ,} \quad (2.1b)$$

$$\text{dynamics: } x \mapsto f(x) = rx(1 - x) + c \ . \quad (2.1c)$$

In the $c = 0$ case, the response diagram is the familiar period-doubling cascade shown in Fig. 1. In the case where $c > 0$ but small, the attractive locus is shifted upward.

Our two-dimensional lattice is an array of 128 by 128 nodes. Further, each node on the left boundary of this square array will be the closest neighbor (to the right) of the corresponding node (at the same height) on the right boundary of the square. Thus, the left and right edges are joined, as a cylinder. Further, the top and bottom edges of the square (or cylinder) are likewise joined. Thus, our lattice is a discretization of the two-dimensional torus. Other topologies could be studied with equal ease, but we have not explored them in this work. At each node, we place one copy of the standard cell, as described in (2.1). The *Laplacian coupling* is defined as follows.

The first control parameter at each node is to be held fixed, at a common value. Thus, for all (i, j) in the range $\{0 \cdots 127\}$,

$$r_{ij} = 4*GN/1000 \ . \quad (2.2)$$

Thus, as GN is fixed at a value between 250 and 1000, all of the first control parameters are fixed at a common value between one and four. The second control parameter at each node is to be determined by Lapacian coupling, which originates from the finite difference method applied to the heat equation. Thus, for all (i, j) in the range $\{0 \cdots 127\}$, the second control parameter at a node is determined by the state at its

node, and the states at the four neighboring nodes according to the coupling scheme defined by the equation

$$c_{ij} = CP^{*}(x_{av} - x_{ij})/1000 \qquad (2.3)$$

where x_{av} is the average value of the current states at the four nearest neighbors, and CP is a constant in the range [0, 1000]. After these couplings, all the coupling parameters of the logistic schemes are bound, but new control parameters, $(CP, GN) \in D \subset \mathbb{R}^2$ have been introduced. These are control parameters of the coupling functions, and we have chosen to fix them on a global basis, rather than to distribute them over the lattice. Thus, the fully coupled lattice is still a dynamical scheme, running on a 16K-dimensional state space, with two control parameters. Although we set these controls only at integer values in our runs, we regard them as real numbers. The values of these control parameters we used, that is, the control space we explored, is shown in Fig. 2.

Finally, we must clip the new state at each node, to maintain its range in the unit interval. Thus, updates

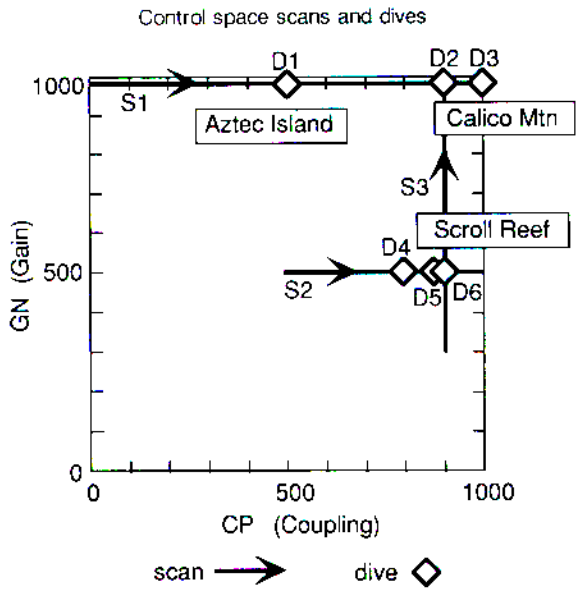

Fig. 2. The Control Space Exploration. After coupling the entire lattice as described in Sec. 2, two parameters remain to be fixed by the experimentalist — the *coupling* and the *gain*. Here we show the plane region of these two parameters. Each diamond icon marks the parameter values of one of our deep-diving experiments, $D1, \ldots, D6$. The black lines with arrows show the path of our scans (S1, S2, and S3.) The labels in boxes identify three regions in which our scans discovered interesting patterns.

at each node are done in the sequence: compute the second coupling parameter via Eq. (2.3), then compute the iteration function via Eq. (2.1c), then clip by the rule:

$$\text{if } f(x) > 1,\ x' = 1\ ; \qquad (2.4a)$$

$$\text{if } f(x) < 0,\ x' = 0\ ; \qquad (2.4b)$$

$$\text{else } x' = f(x)\ . \qquad (2.4c)$$

Then, replace x by x' and resume. This method of clipping is crude but effective.

3. The MPP and the Blue Room

Until recently, the MPP was a one-of-a-kind supercomputer. Now there are a growing number of MPP-type devices. Maintained by the Space Data and Computing Division of the NASA Goddard Space Flight Center for research purposes, it consists of 16K processors connected in a two-dimensional array, 128 by 128. It is accessible over a global DECnet, and is programmed via MFORTH, a FORTH compiler for the MPP written by one of us (JED). The FORTH code producing the results described in this paper is about thirty lines long! Our toral logistic lattice is a natural fit to the architecture of the MPP, and our implementation utilizes 20 bit fixed point arithmetic. The range, approximately -8 to $+8$, is covered evenly with one sign bit, three integer bits, and 16 fraction bits. Thus, the state space [0, 1] is covered by 64K numbers. A run of one million iterations of the cellular dynamical system takes about 45 minutes, at about 1100 iterates per second. More precise arithmetic, and larger lattices, may easily be accommodated by small changes in the program. We chose these values to obtain a good speed for our preliminary exploration.

The current state of the lattice may be viewed conveniently on a personal computer or graphics terminal located anywhere on the network. (We are using a Apple Macintosh II). We worked in the *Blue Room*, the control room of the MPP. This is equipped with a Panasonic optical disk video recorder and other video peripherals ideal for our project. We were able to record long sequences of states, and then to examine them frame by frame, or at various speeds. The MPP was able to compute thousands of iterates in the time it took us to draw one state on the color monitor and examine it. Thus, we were able to zoom through the three-dimensional space of control parameters (CP, GN) and iteration number, I, at high speeds. The screen images were displayed with a rainbow palette of

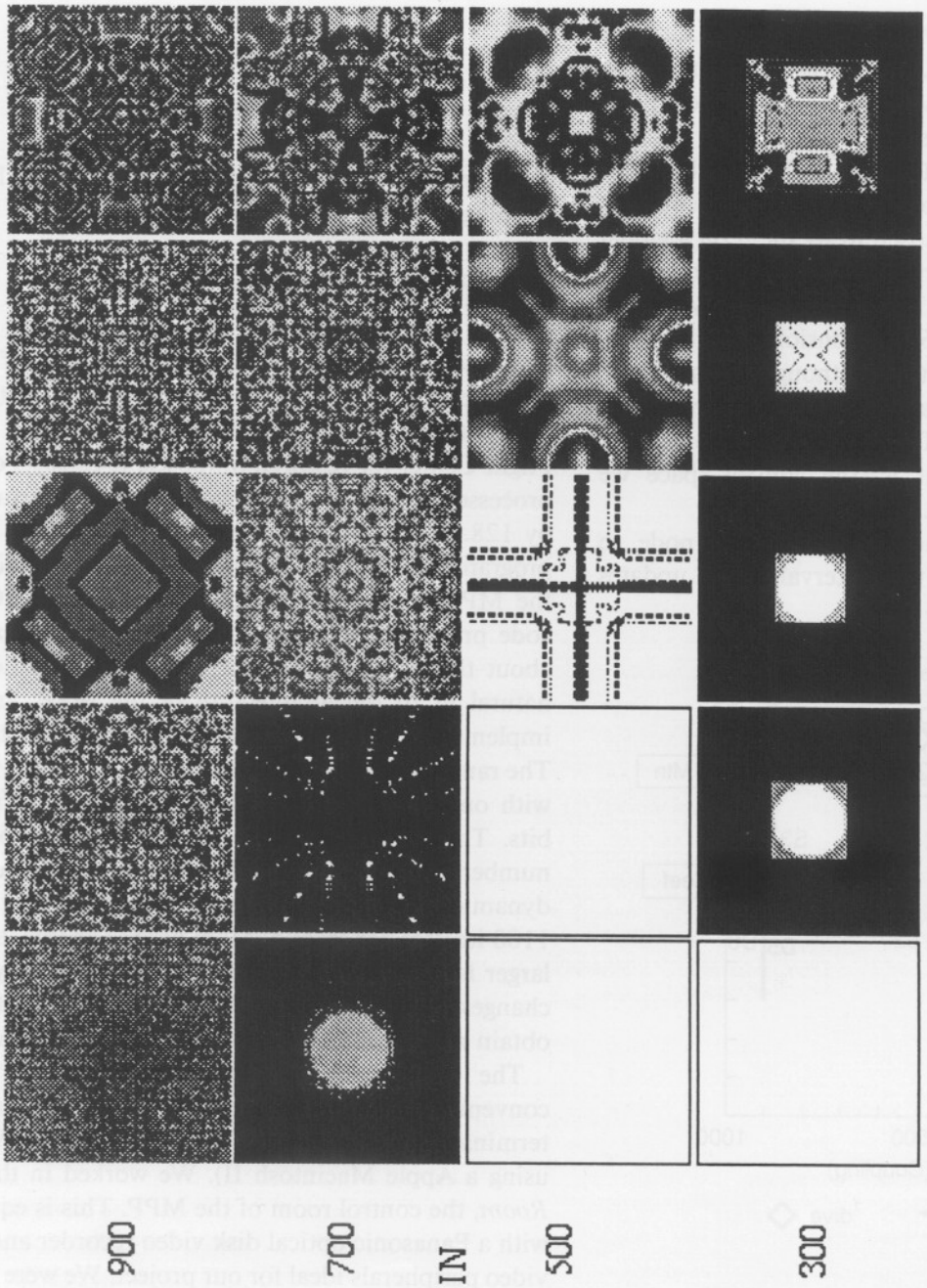

Fig. 3. The 1000-iteration plane. Here, against a background of the control plane described in Fig. 2, we show a tableau of patterns found at twenty points in the control plane. Each pattern is the 1000th iterate beginning with the circular initial pattern.

256 colors representing the interval [0, 1], with black at zero, through shades of blue and green, ending at one with red.

4. Findings

Our initial observations regard the relationship between macroscopic patterns and periodicity. With the gain, *GN*, at the larger values (900 or so), the individual nodes are usually chaotic. Nevertheless, large-scale organization is observed when the coupling strength, *CP*, is sufficiently strong (500 or more). We thought of the control parameter rectangle, *C*, as a patch of ocean, and the MPP as a submarine in which we could descend rapidly to unexplored depths. We scanned just below the surface, at a depth of about a thousand iterations ($I = 1$K). Most of this layer appeared chaotic. We made test dives to 50K wherever we liked.

The initial condition used in this preliminary survey of the phase space is a large symmetrical central disk of 0.22 gray on a very light 0.05 background. As a result, this study produced symmetrical patterns, as shown in Fig. 3. A random initial condition produced rather different results, as shown in Figs. 4 and 5.

A sense of territory is provided by Fig. 3, which shows the 1000th iterate at intervals of 200 in gain (GN) and coupling (CP). With depth, we found that chaotic transients sometimes persisted past a million iterations, then settled down to a periodic attractor. As the dynamics occurs in a vector space of dimension 16K, it is not always easy to recognize periodicity. We have built tools to automate these perceptions. The scans and dives we have recorded, indicated on the phase space map of Fig. 2, are as follows.

Scan 1. This is a west-to-east scan at a depth of 1K, in the far north of the patch, at high gain, $GN = 990$, as shown in the map in Fig. 3. After extensive travels through a terrain of chaotic mandalas, we encountered recognizable patterns with *CP* values from about 478 to 585. We named this *Aztec Island*. Continuing through another vast plateau of chaos, we found another ordered regime, *Calico Mountain*, with *CP* from about 875 to 1000.

Scan 2. Another west-to-east scan at a depth of 1K, this time in the central region, $GN = 500$. This begins with a static attractor (all black) which persists from the start, $CP = 0$, until almost 700. Then we burst into *Scroll Reef*, a large regime of patterns with robust personality. This extends to about CP = 970.

Scan 3. Here we scanned from the southern border northward in the far eastern territory, with $CP = 900$, again at depth 1K. Patterns begin around $GN = 350$. Besides the difficult-to-grasp chaos, we passed again through Scroll Reef, attaining Calico Mountain at $GN = 660$.

All these features are shown on the map in Fig. 2. Next we did some diving. The six dives we recorded are also shown on the map.

Dive 1. Aztec Island, at (500, 990). We started down here to see what the dynamics of the Aztec patterns looked like. We found rapid convergence to a period-eight attractor, within 2K iterations.

Dive 2. Scans 1 and 3 cross on Calico Mountain. We dove here at this crossing, (900, 990), from the surface to our scan depth, and found rapid convergence to a periodic attractor of period six. The Calico pattern was very robust. (Later, we double-checked this. Diving beyond 2K, we were surprised to see that this faded to a static attractor by $I = 2250$.)

Dive 3. Slightly to the east of Dive 2, at (1000, 990), we found convergence to a period-two attractor at a depth of 5K.

Dive 4. Sailing south to Scroll Reef, we dove at (800, 500), the crossing of Scan 2 and Scan 3. Here we found a period-eight checkerboard at a depth of 5K.

Dive 5. A bit to the east, at (890, 500) in Scroll Reef, we found a period-18 checkerboard at a depth of 12K. All three of our initial conditions converged to this same attractor.

Reminiscent of the paintings of Marc Rothko, this was one of our most beautiful dynascapes.

Dive 6. Very nearby, at (900, 500) in Scroll Reef, we dove again, expecting another periodic dynascape. We found a sort of convergence around 200K, but no obvious period. We dove as deep as we could, well past two million iterations, without discovering a periodic cycle. We observed a vague period of nine, an almost period of 28, a near period of 768. Below depth 2M, we verified that there was no period shorter than four thousand iterations.

5. The Video

Some of the runs described above have been recorded on a video cassette. We recorded these at a rate of 10 frames per second (except Scan 1, at 30 frames per second), as this seemed the fastest we could watch without getting seasick. But the frames are not consecutive iterations. We usually strobed the periodic attractors, so that the entire convergence could be observed without flicker. Here are the captions for the video sequences.

Scan 1. West to east at $GN = 990$, through Aztec Valley and Calico Mountain. In single steps, *CP* increases from 0 to 1000, 33 seconds.

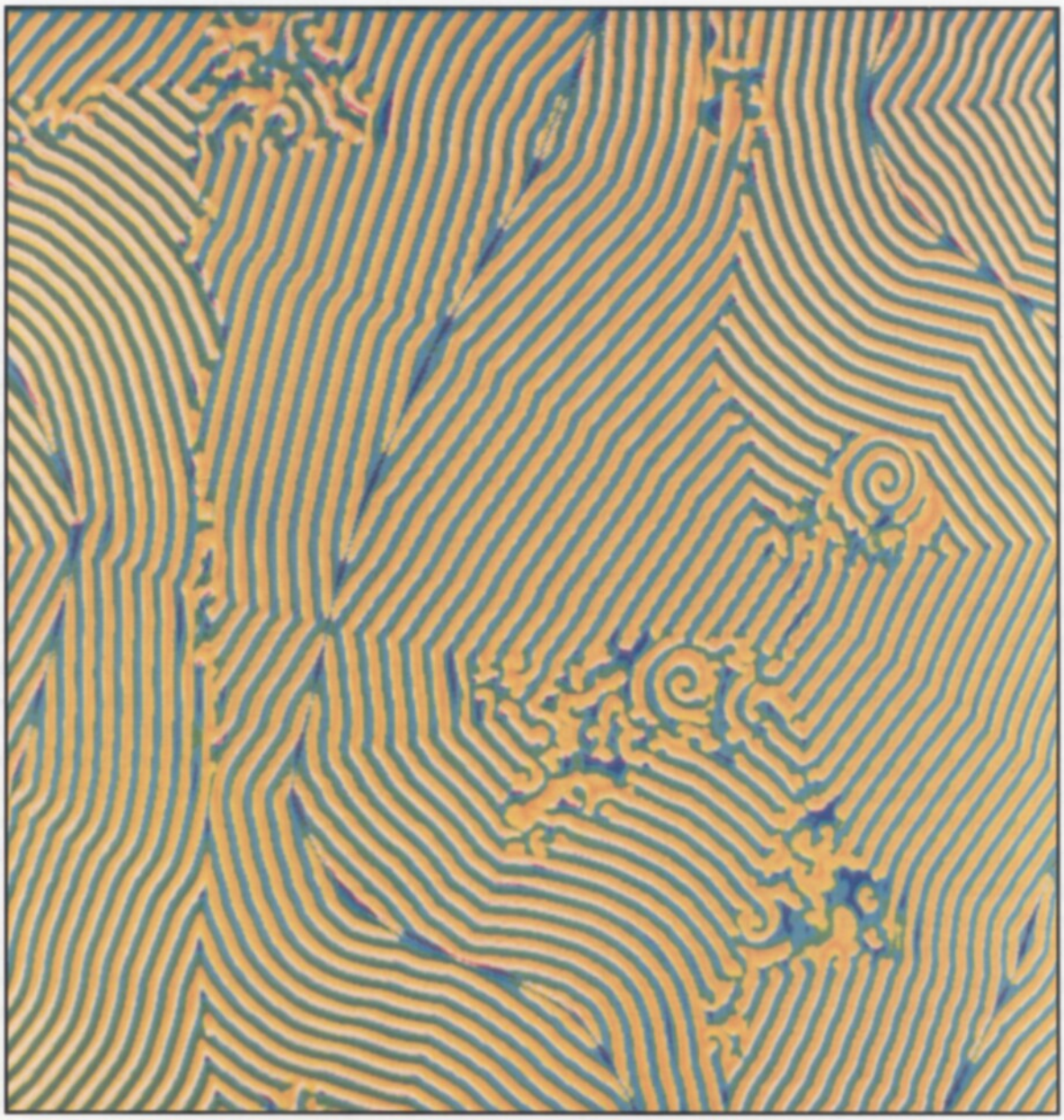

Fig. 4. Scroll Reef, 512 × 512, random initial state, 40K deep. Here, for comparison, is an image from the larger lattice, starting with a random initial pattern, and diving to a depth of 40 000 iterations. The control point, in Scroll Reef, is near the point *D*6 on Fig. 2.

Fig. 5. Aztec Island, 512×512, random initial state, 8K deep. Similar to Fig. 4, but with control point in Aztec Island, near $D1$ on Fig. 2, and diving only to 8000 iterations.

Scan 2. West to east at $GN = 500$, through Scroll Reef. In steps of five CP increases from 500 to 1000, 10 seconds.

Scan 3. South to north, at $CP = 900$, through Scroll Reef and Calico Mountain. In steps of two, GN increases from 400 to 1000, 30 seconds.

Dive 1. Aztec Valley, (500, 990), dive to depth 2K in steps of eight, converging to the strobed attractor of period eight in 25 seconds.

Dive 2. Calico Mountain, (900, 990), dive to depth 900 in steps of six, converging to the strobed attractor of period six in 15 seconds.

Dive 6. Scroll Reef, (900, 500), dive to 1.56M in five stages, 2.5 minutes.

a) 20 frames of 1K steps
b) 18 frames of 10K steps
c) 80 frames of 28 steps
d) 1200 frames of single steps
e) 160 frames of 768 steps

Then back up to a depth of 6000 iterations to look at the scrolls at 1 and then 8 iterations per frame.

6. Conclusions

More work is needed to explore the full territory of the two-dimensional toral logistic lattice with Laplacian coupling. The availability of a machine capable of more than 1K steps per second, along with digital video recording on optical disk and direct transfer to the color screen of a Macintosh II, makes such an exploration practical. We hope, in time, to explore further, with automatic tools for identifying periodic phenomena, and for the quantification of spatio-temporal chaos. Extension of the FORTH code to 512 by 512 lattices has been completed and preliminary results are shown in Figs. 4 and 5.

Acknowledgements

It is a pleasure to acknowledge the support of Milton Halem, Chief of the Space Data and Computers Division, Jim Fischer, head of the Computer Systems Research Facility, and Gerald Soffen, Associate Director for Space and Earth Sciences, all of NASA Goddard Space Flight Center. Madonna Turner, a summer intern at Goddard, participated in the program development. Also, we are grateful to Jim Crutchfield, Kuni Kaneko, Rob Shaw, and Gottfried Mayer-Kress for their pointers and encouragement.

References

Abraham, R. H. & Shaw, C. D. [1982–88] *Dynamics, the Geometry of Behavior* (four volumes) (Aerial Press, Santa Cruz, CA).

Abraham, R. H. [1986] "Cellular dynamical system", in *Mathematics and Computers in Biomedical Applications, Proc. IMACS World Congress. Oslo, 1985*, eds. Eisenfeld, J. & DeLisi, C. (North-Holland, Amsterdam) pp. 7–8.

Crutchfield, J. P. [1984] *Space-Time Dynamics in Video Feedback and Chaotic Attractors of Driven Oscillators* (video tape) (Aerial Press, Santa Cruz, CA).

Crutchfield, J. P. & Kaneko, K. [1987] "Phenomenology of spatio-temporal chaos", in *Directions in Chaos*, ed. Hao, B.-L. (World Scientific, Singapore).

Devaney, R. L. [1989] *An Introduction to Chaotic Dynamic Systems*, second ed. (Addison-Wesley, Reading, MA).

Fisher, R. A. [1930/1958] *The Genetical Theory of Natural Selection* (Dover, New York).

Kaneko, K. [1989] "Spatiotemporal chaos in one- and two-dimensional coupled map lattices", *Physica* **37D**, 60–82.

Kapral, R. [1986] "Discrete models for the pattern formation and evolution of spatial structure in dissipative systems", *Phys. Rev.* **A33**, 4219–4231.

May, R. [1976] "Simple mathematical models with very complicated dynamics", *Nature* **261**, 459–467.

Shaw, R. S. [1988] *Split* (film) (Starker Films, Santa Cruz, CA).